sciendo

POLISH MARITIME RESEARCH 4 (104) 2019 Vol. 26; pp. 47-55
10.2478/pomr-2019-0065

A METHOD TO DETERMINE THE TIGHTENING SEQUENCE FOR STANDING RIGGING OF A MAST

Leszek Samson
Gdańsk University of Technology, Poland
Maciej Kahsin
Gdańsk University of Technology, Poland

ABSTRACT

The article proposes an alternative method to determine the sequence of generation of pre-tension forces in standing rigging of a mast. The proposed approach has been verified on both a virtual simulation experiment and laboratory tests. In this method, the desired tension values are obtained using the influence matrix which allows to calculate the effect of tension change in an individual rope on the tension distribution in the remaining ropes in the system. Unlike the presently used method, in which the desired tension distribution is obtained in a long-lasting iterative process burdened with relatively large errors of final values, the proposed method makes it possible to achieve the final tension distribution in a finite number of steps. In the case of FEM analyses, the new method can be a useful tool for determining an arbitrary distribution of tension forces in ropes via solving a system of linear equations.

Keywords: pre-tension,standing rigging,rig,tightening sequence,initial tension

INTRODUCTION

Guy rope systems are used in numerous technical objects in which achieving an appropriate force distribution is of high importance. A sample list of such objects may include: suspension bridges, drawbridges, and guyed masts and chimneys. This paper analyses the tension distribution issue for a guyed mast.

Classification societies require that the pre-tension in standing rigging is periodically controlled and that the tension forces in ropes are equal to those predicted by the designer [1, 2, 14].

The tightening sequence for a standing rigging should be properly planned, as an incorrect sequence of tightening may lead to damage, or even total deterioration of the object [3, 10, 19].

The requirements of classification societies do not provide recommendations concerning proper selection of tension force generation sequence. Also, there are no literature publications which would study and attempt to optimise the above task in maritime applications.

The presently used method consists in achieving the desired tension in a rope via tightening individually each element of the rigging, each time adapting the tension force

to the desired value, until the satisfactory force distribution is obtained [7, 9]. In this article, the above approach is referred to as the standard method.

Due to mutual interaction between the ropes and with the remaining elements of the structure, the above method takes, as a rule, an iterative course, which makes achieving the predicted tension distribution practically impossible [4, 5, 6, 8, 11, 15, 18].

The new method proposed in the article makes use of the influence matrix [16, 17] and the initial tension distribution in the ropes. This approach makes it possible to achieve the desired force distribution in a limited number of steps.

The above two methods are compared in the article based on the results of simulation studies and experimental tests.

The new method is based on a system of linear equations, the coefficients of which are the elements of the influence matrix. It is assumed that the ropes are rectilinear before and during the tightening process and, consequently, the matrix elements do not change their values.

TESTED OBJECT

The object used for comparing the standard method and the new method is a mast with three guy ropes. Fig. 1 shows a sketch of the structure, where elements 1 through 3 represent the ropes and element 4 is the mast.

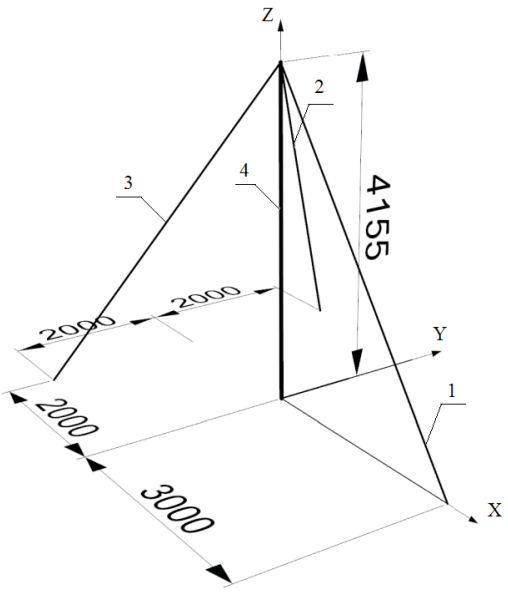

Fig. 1. Sketch of mast with three guy ropes, dimensions in [mm]

TEST RIG

The mast is made of aluminium alloy. Its cross-section has the shape of circular ring with outer diameter of 60 mm and wall thickness of 2.5 mm. The mast was welded to a plate of 25 mm in thickness, made of aluminium alloy, and then the entire structure was screwed to the base.

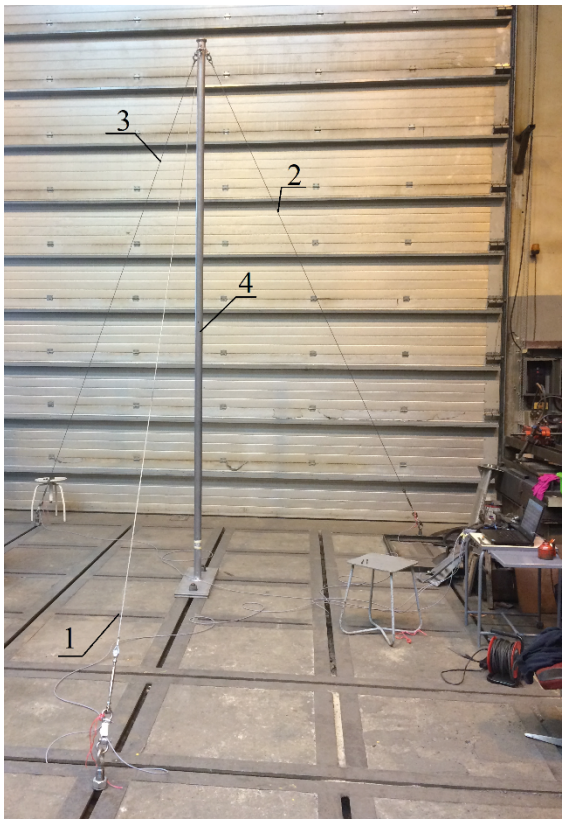

Fig. 2. Test rig: 1,2,3 – guy ropes, 4 – mast

Galvanised steel ropes 6x19+FC with diameter of 5 mm were fastened with hooks to the masthead and with anchor bolts to the floor. Between each hook and anchor bolt there were: the rope, a tightener, a dynamometer, and shackles. Details of the test rig are shown in Fig. 3 and Fig. 5. The prepared test rig made it possible to measure the tension force in a rope with the accuracy of up to 4 N.

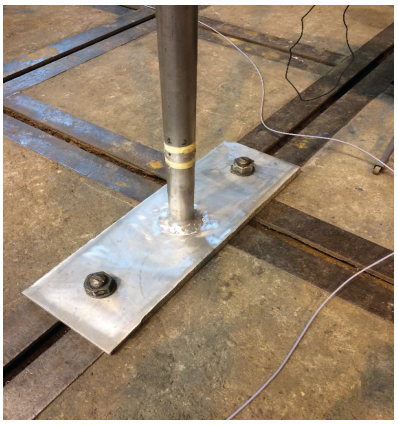

a) mast base *b) anchor bolt*

Fig. 3. Details of mast attachment

FEM MODEL

To verify qualitative advantages of the new method over the standard method, a numerical simulation study was performed. The model of the real mast structure was discretised using the Final Element Method (FEM). In the further step of the study, the results of the simulation were compared with those measured on the real test rig.

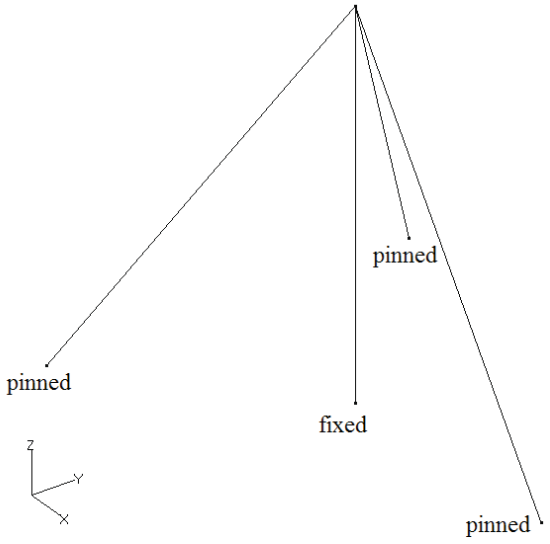

Fig. 4. The applied discrete model and boundary conditions

In the numerical model, the ropes and the mast were modelled as one-dimensional elements: rods and beam, respectively. The parameters of the discrete elements reflected the characteristics of the real object.

The material characteristics were determined experimentally using a testing machine. For aluminium alloy, the obtained longitudinal modulus of elasticity was equal to 67 GPa. The equivalent stiffness assumed for the rope-tightener-dynamometer-shackle unit corresponded to the circular cross-section of 5 mm in diameter and the longitudinal modulus of elasticity equal to 50 GPa. This representation of stiffnesses made it possible to model the entire guy rope unit as one finite element.

The numerical model consists of four finite elements. As the boundary conditions, all degrees of freedom were removed at the mast base, along with all linear displacements of the ropes fastened to the floor. The numerical model is shown in Fig. 4.

The masthead model was simplified: the node was situated at the intersection of straight lines between the rope attachment points and the mast axis.

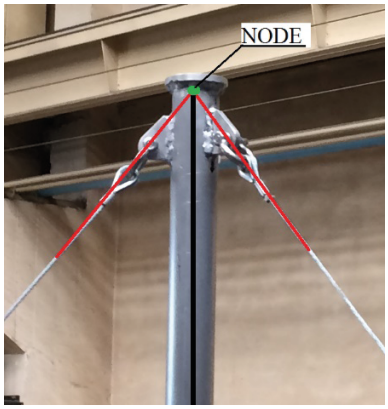

Fig. 5. Fastening of guy ropes to the masthead

The tension forces in the ropes were generated by shortening of the rod element modelling the real rope [12, 13]. Equivalent rope shortening and force generation was achieved via a temperature change and the resulting response of the structure. The desired force value in the element was achieved in two steps. In the first step, the force change in the element which resulted from the temperature change by 1 degree was generated and recorded. Then, in the second step, assuming structural linearity, the temperature increase was calculated which was necessary to achieve the desired total force change in the element.

STANDARD METHOD

In the standard method, the process starts from an arbitrary rope in which the tension force is tuned to the desired value via shortening, or lengthening, of the rope with the tightener. In the next step, the tension force in the next rope is tuned, and so on, until the desired tension distribution is achieved in the entire rigging.

The set of the desired tension forces can have the following vector form:

$$\mathbf{S}_{\mathbf{des}} = \begin{Bmatrix} 700 \\ 514 \\ 514 \end{Bmatrix} N \qquad (1)$$

This vector, the same for all cases, was assumed in the analysis presented in the article.

To illustrate the method, the rope tightening process was simulated numerically and studied experimentally in the test rig. The process started from rope 1 (acc. to Fig.1), in which the tension force was tuned to 700N, then the force of 514N was generated in rope 2, and finally, the force in rope 3 was corrected to 514N. In the next iterations, these actions were repeated.

The initial distribution of tension forces in the ropes can be given as the following vector (with the row number corresponding to the rope number):

$$\mathbf{S}_{init} = \begin{Bmatrix} 208 \\ 142 \\ 125 \end{Bmatrix} N \quad (2)$$

In the standard method, the information on the initial force distribution in the ropes is not necessary. The method starts with an arbitrary rope. Therefore, the initial force distribution does not affect the sequence of actions when tightening the structure.

Fig. 6 shows force changes in the ropes which were recorded experimentally after each of 12 tightening steps (which in total corresponded to 4 iterations). Step 0 represents the initial force distribution.

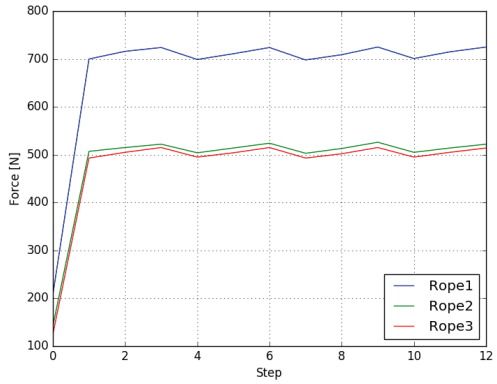

Fig. 6. Changes of forces in ropes: experiment, standard method, 12 tightening steps

The results obtained after the last tightening step (step 12) are given in Table 1.

Tab. 1. Force values in ropes recorded experimentally after 12 tightening steps: standard method

Rope	Desired value [N]	Obtained value [N]	Difference [%]
1	700	725	3.6
2	514	522	1.8
3	514	514	0.0

The course of the tightening process simulated using the FEM model is shown in Fig. 7.

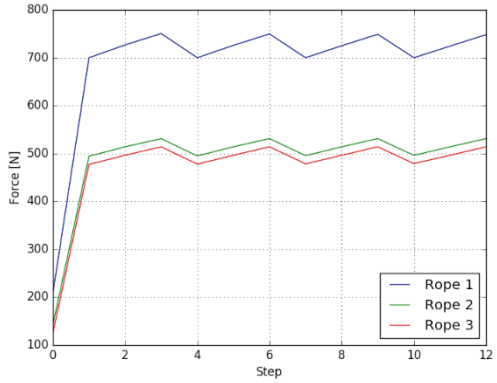

Fig. 7. Changes of forces in ropes: FEM simulation, standard method, 12 tightening steps

The results of simulation after tightening step 12 are given in Table 2.

Tab. 2. Force values in ropes obtained from FEM simulation after 12 tightening steps: standard method

Rope	Desired value [N]	Obtained value [N]	Difference [%]
1	700	748	6.9
2	514	531	3.3
3	514	514	0.0

Fig. 8 shows the result of the simulation for the standard method, when the tightening sequence was extended to 82 steps. It is clearly visible that, even for such a long time of tightening, the desired tension distribution has not been obtained. The final force values in individual ropes after step 82 are given in Tab. 3.

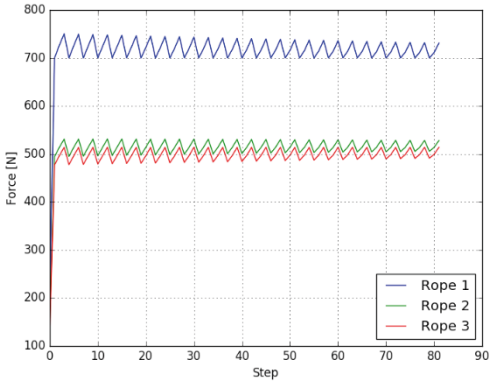

Fig. 8. Changes of forces in ropes: FEM simulation, standard method, 82 iterations,

Tab. 3. Force values in ropes obtained from FEM simulation after 82 iterations: standard method

Rope	Desired value [N]	Obtained value [N]	Difference [%]
1	700	731	4.5
2	514	528	2.8
3	514	514	0.0

METHOD MAKING USE OF INFLUENCE MATRIX

The method proposed in this article makes use of the influence matrix **A**, the initial force vector $\mathbf{S}_{init}$, and the desired force vector $\mathbf{S}_{des.}$

Matrix **A** is a square matrix with the dimension equal to the number of ropes. In each row, the matrix elements represent force changes in ropes generated by the elementary force increase in the rope corresponding to the row number. For instance, row 1 is created as a result of elementary force increase in rope 1, therefore the first element is equal to 1

and the remaining elements correspond to the resulting force changes in the other ropes.

The desired force vector can be calculated from Eq. (3):

$$\mathbf{S}_{des} = \mathbf{S}_{init} + \mathbf{A}\,\Delta\mathbf{S} \tag{3}$$

where ΔS is the force increase vector, in which successive rows correspond to rope numbers.

Transforming this equation gives Eq. (4):

$$\Delta\mathbf{S} = \mathbf{A}^{-1}(\mathbf{S}_{des} - \mathbf{S}_{init}) \tag{4}$$

The obtained vector ΔS contains the force increase values which should be generated to achieve vector $\mathbf{S}_{des.}$

Solving Eq. (4) requires that the influence matrix **A** is a nonsingular matrix, which is fulfilled for statically indeterminate systems.

EXECUTION OF NEW METHOD

The influence matrices have been determined separately for the examined real object and the simulation model.

The experimentally obtained influence matrix is given as:

$$\mathbf{A}_{eks} = \begin{bmatrix} 1.0 & 1.349 & 1.326 \\ 0.723 & 1.0 & 0.962 \\ 0.732 & 0.986 & 1.0 \end{bmatrix} \tag{5}$$

while the influence matrix for the discrete model is:

$$\mathbf{A}_{MES} = \begin{bmatrix} 1.0 & 1.352 & 1.352 \\ 0.716 & 1.0 & 0.968 \\ 0.716 & 0.968 & 1.0 \end{bmatrix} \tag{6}$$

The initial force vector was:

$$\mathbf{S}_{init} = \begin{Bmatrix} 245 \\ 173 \\ 196 \end{Bmatrix} N \tag{7}$$

Based on the experiment, the force increase vector ΔS was calculated from Eq. (4) as:

$$\Delta\mathbf{S} = \begin{Bmatrix} 362 \\ 572 \\ -512 \end{Bmatrix} N \tag{8}$$

The following tightening sequence was assumed:
- in rope 1: tension force was increased by 362 N,
- in rope 2, tension force was increased by 572 N,
- in rope 3, tension force was decreased by 512 N.

Fig. 9 illustrates the force values obtained when executing the force increase vector (8).

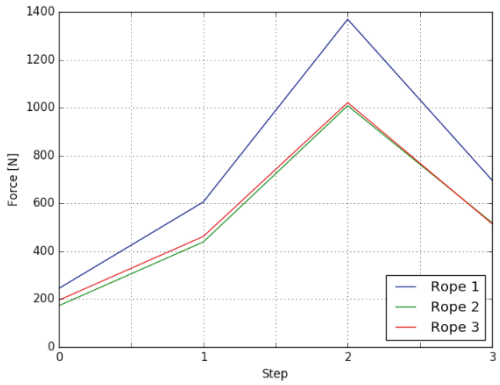

Fig. 9. Changes of forces in ropes: experiment, new method, 3 tightening steps

Table 4 collates the force values in the ropes, which were achieved after tightening step 3.

Tab. 4. Absolute rope tension force error experimentally recorded after 3 tightening steps: new method

Rope	Desired value [N]	Obtained value [N]	Difference [%]
1	700	697	-0.4
2	514	519	1.0
3	514	514	0.0

The vector ΔS was calculated using Eq. (4) and the influence matrix (6) obtained from FEM simulation:

$$\Delta\mathbf{S} = \begin{Bmatrix} 159.3 \\ 484.7 \\ -265.3 \end{Bmatrix} N \tag{9}$$

Fig. 10 illustrates changes of forces in ropes after successive tightening steps.

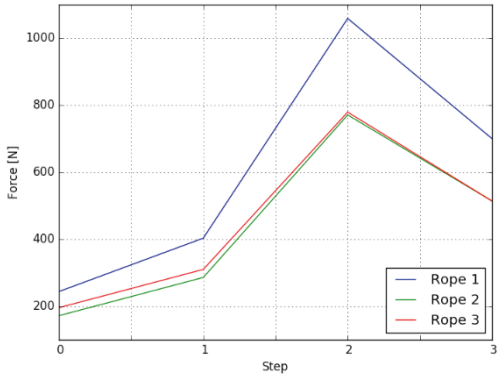

Fig. 10. Changes of forces in ropes: FEM simulation, new method, 3 tightening steps

Table 5 collates the force values in the ropes, which were achieved after 3 tightening steps.

Tab. 5. Force values in ropes after 3 tightening steps: FEM simulation, new method

Rope	Desired value [N]	Obtained value [N]	Difference [%]
1	700	700	0.0
2	514	514	0.0
3	514	514	0.0

LIMITS IN APPLICATION OF NEW METHOD

The new method is based on linear relationships between loads, displacements, and deformations. To ensure preservation of constant values of the influence matrix elements, certain limits were introduced with respect to minimal and maximal forces in ropes during the tightening process.

MINIMUM FORCE LIMIT

To limit possible effects caused by rope loosening, the tension forces in ropes should not drop below zero. In the present analysis, the intransgressible minimum limit for forces in ropes was assumed equal to 150 N.

Based on the numerical analysis, the initial force vector for the examined rope system was selected as:

$$\mathbf{S}_{init} = \begin{Bmatrix} 250 \\ 180 \\ 180 \end{Bmatrix} N \tag{10}$$

The force increase vector was calculated from Eq. (4) as:

$$\Delta\mathbf{S} = \begin{Bmatrix} -549 \\ 369 \\ 369 \end{Bmatrix} N \tag{11}$$

Fig. 11 shows the predicted tightening sequence for which the forces in all ropes drop below the assumed limit in the first iteration step.

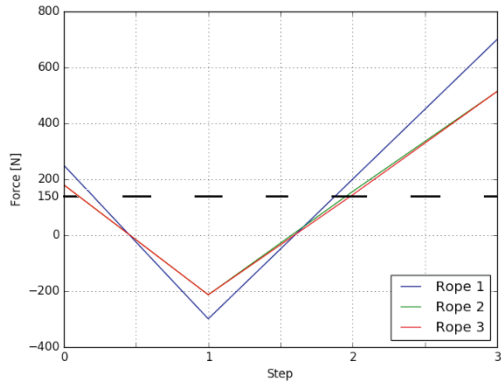

Fig. 11. Unacceptable tightening sequence due to force drop in all ropes below the assumed limit

In such a case, it is necessary to terminate the tightening step before the tension force in any rope drops below the assumed limit.

To execute the force increase vector (11), in the first step, the force drop by 42 N was generated in rope 1, which led to force increase by 150 N in ropes 2 and 3. Then, in the second and third steps, the forces in rope 2 and rope 3 were increased by 369 N, respectively. In the final, fourth step, the force in rope 1 was decreased by 507 N, (being the difference between the desired force of -549 N and the force -42 N applied in the first step).

The tightening executed in accordance with the above sequence does not lead to force dropping below the assumed low limit in any rope. The corrected tightening sequence is illustrated in Fig. 12.

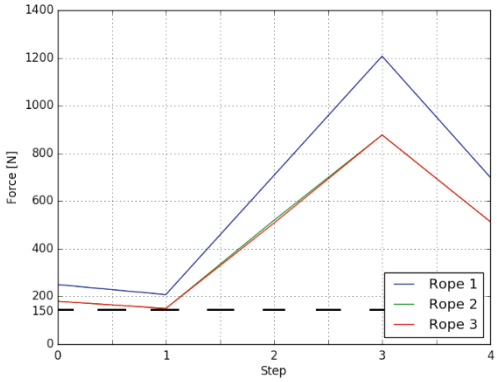

Fig. 12. Rope tightening sequence taking into account the minimum force criterion

MAXIMUM FORCE LIMIT

To ensure a safe sequence of rope tightening, it is necessary to introduce a maximum limit for forces in ropes which must not be exceeded during the tightening. This limit can be determined by a maximum permissible load of the rope, or some equipment elements, and/or by the carrying capacity limit of the used measuring sensors. The maximum limit for tension forces in ropes assumed in the present analysis was equal to 1300 N.

The effect of exceeding this limit was tested on the case with the initial force vector:

$$\mathbf{S}_{init} = \begin{Bmatrix} 210 \\ 175 \\ 175 \end{Bmatrix} N \tag{12}$$

The force increase vector ΔS was calculated using Eq. (4) and the influence matrix (6) obtained from FEM simulation:

$$\Delta\mathbf{S} = \begin{Bmatrix} 1492 \\ -371 \\ -371 \end{Bmatrix} N \tag{13}$$

Fig. 13 shows the predicted tightening sequence, for which the tension force in rope 1 exceeds the assumed limit in the first iteration step.

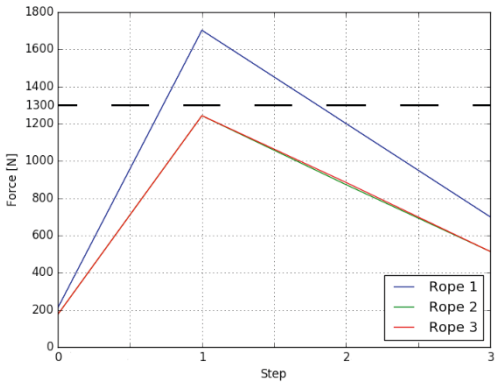

Fig. 13. Unacceptable tightening sequence due to exceeding maximum force limit in rope 1

Analogously to the case of minimum force in rope, the tightening step should be terminated before the maximum force limit is exceeded in any rope.

For the analysed case, in the first step, the force in rope 1 should be increased by 1492 N, but this would lead to exceeding the assumed force limit of 1300 N. Therefore, the force in this rope can only be increased by 1090 N to reach the limit. In the second and third steps, the tension forces were decreased by 371 N in rope 2 and rope 3, respectively. In the final step, the force in rope 1 was increased again, this time by 402 N, being the difference between the desired force value of 1492 N and the previously applied force increase of 1090 N. Using the above tightening sequence, the desired tension force distribution was obtained after four steps, without exceeding the assumed maximum force limit. The course of force changes in ropes for this case is illustrated in Fig. 14.

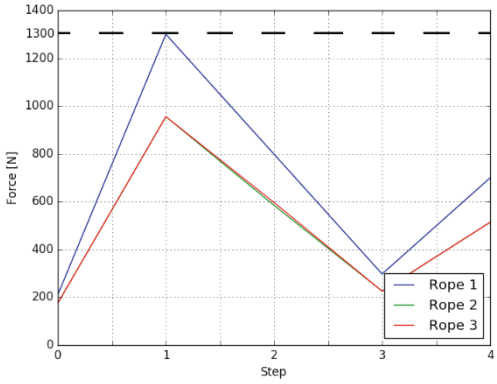

Fig. 14. Corrected tightening sequence taking into account the maximum force limit

TESTING MINIMUM AND MAXIMUM FORCE LIMITS IN ROPES

An experiment was performed on a test rig to check the effect of minimum and maximum limits imposed on tension forces in ropes. The exact values of these limits were equal to 150 N and 1300 N, respectively.

The initial force distribution in ropes was:

$$\mathbf{S}_{\mathbf{init}} = \begin{Bmatrix} 315 \\ 240 \\ 247 \end{Bmatrix} N \tag{14}$$

Using Eq. (4), the vector ΔS was calculated for the influence matrix (5) and the initial force distribution (14):

$$\mathbf{\Delta S} = \begin{Bmatrix} 1984 \\ -559 \\ -638 \end{Bmatrix} N \tag{15}$$

Generating the force increase of 1984 N in rope 1 is not possible, as it would lead to exceeding the maximum force limit. Therefore, in the first step, the tension force in rope 1 was increased by 985 N to reach the limit of 1300 N in this rope. In the second step, the force in rope 2 was decreased by 559 N. Then, in the third step, the force in rope 3 was decreased by 253 N, as the tension force in rope 2 reached the minimum limit of 150 N. In the fourth step, the force in rope 1 was increased by 999 N, being the difference between 1984 N (the desired final value) and 985 N (the force change applied in the first step). In the fifth step, no action was taken in rope 2, as the entire force change was already generated in the second step. In the final, sixth step, the tension force in rope 3 was decreased by 385 N, being the difference between the desired final value of -638 N and the force decrease by 253 N executed in the third step.

The above tightening sequence is shown in Fig. 15.

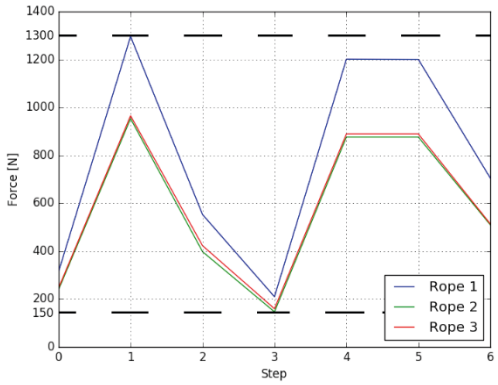

Fig. 15. Changes of forces in ropes taking into account assumed force limits: experiment, new method, 6 tightening steps

The values of forces in individual ropes obtained after 6 tightening steps are collated in Table 6.

Tab. 6. Force values in ropes experimentally recorded after 6 tightening steps: new method

Rope	Desired value [N]	Obtained value [N]	Difference [%]
1	700	705	0.7
2	514	510	-0.8
3	514	514	0.0

CONCLUSIONS

The article compares two methods of structure tightening applied to a guyed mast, namely: the currently used standard method, and the new method proposed by the authors. Laboratory tests and FEM simulations were performed to assess the number of steps needed to achieve the desired force distribution in the ropes composing the examined rigging structure.

The proposed method radically simplifies the optimal tightening procedure for a given rigging to obtain the desired tension distribution in ropes. It makes it possible to obtain, in a small number of steps, accurate values of pre-tension forces using a numerical model. In the conventional iterative approach, this task was extremely time and labour consuming.

The differences between the values of influence matrix elements for the numerical model (5) and the real physical object (6) amount to 2.5% of absolute error. Possible causes of these differences will be analysed to create a more accurate numerical representation of the real object, and thus to allow direct application of the influence matrix obtained from FEM simulation to real objects.

The obtained results have shown that the proposed method makes it possible to control tension forces in ropes, and to obtain the desired tension distribution in a given rigging. Practical implementation of this method requires taking into account real limits concerning the stability of the structure and intransgressible minimum and maximum tension limits in its elements. These two aspects are the object of current studies performed by the authors.

BIBLIOGRAPHY

1. DNV GL, Rules for Classification.: *Design and construction of large modern yacht rigs,* 2016.
2. Lloyd's Register., Rules and Regulations for the Classification of Ships.: *Masts and standing rigging*, Part 4, Section 10, 2017.
3. Ślęczka D., Ziemiański L.,: *Dynamic response of the mast to rapid break of guy rope (in Polish)*, Budownictwo i Inżynieria Środowiska, 45, 2007.
4. Grabe G.: *The Rig of the "UCA" - Finite element Analysis,* University of Applied Sciences, Amsterdam 2004.
5. Grabe G.: *The Carbon and PBO Rig for the "sailOvation" - Finite element Analysis,* University of Applied Sciences, Kiel.
6. Grabe G.: *The Rig of the research sailing yacht "Dyna" Measurements of Forces and FEA,* High Performance Yacht Design Conference, Auckland-New Zealand 2002.
7. Rizzo C., Boote D., *Scantling of mast and rigging of sail boats: A few hints from a test case to develop improved design procedures,* 11th International Symposium on Practical Design of Ships and Other Floating Structures, Brazil 2010.
8. Bentes J., Menezes R., Riera J.: *Dynamic response of guyed towers in transmission lines submitted to broken conductors,* 9th International Conference on Structural Dynamics, Portugal 2014.
9. Nelofer A., Kumar S.: *Finite Element Analysis of Guyed Masts under Seismic Excitation*, International Journal of Science and Research 2015.
10. Cuomo A., Zucker H., Dreslin S.: *Tower Technician Killed When Guyed Tower Collapsed, Case Report 09NY095,* Fatality Assessment and Control Evaluation, New York-USA 2017.
11. Hensley G., Plaut R.: *Three-dimensional analysis of the seismic response of guyed masts,* Engineering Structures 29, 2006.
12. ADINA R&D Inc. *Theory and Modeling Guide,* Watertown, MA, USA,2009
13. NX Nastran, *Theoretical Manual,* 2016.
14. Bureau Veritas, *Rules for the Classification and the Certification of Yachts,* NR500, 2016
15. Kozioł K., *Guyed bar structures: the analysis of dynamic response to exceptional loads (in Polish),* Politechnika Krakowska, Kraków 2007.
16. Coria I., Abasolo M., Olaskoaga I., Etxezarreta A., Aguirrebeitia J.: *A new methodology for the optimization of bolt tightening sequences for ring type joints,* Ocean Engineering 129, 2017, pp.441–450.
17. Yu-wen D., You-yuan W.: *A Research to Cable Force Optimizing Calculation of Cable-stayed Arch Bridge,* Procedia Engineering 37, 2012, pp.155 – 160.
18. Bradon J., Chaplin C., Ermolaeva N.: *Modelling the cabling of rope systems*, Engineering Failure Analysis 14, 2007, pp.920–934.
19. Kozak J., Tarełko W.: *Case study of masts damage of the sail training vessel POGORIA*. Engineering Failure Analysis, Volume 18, Issue 3, 2011, pp.819-827.

CONTACT WITH THE AUTHORS

Leszek Samson
e-mail: leszek.samson@pg.edu.pl
Gdańsk University of Technology,
Gabriela Narutowicza Street 11/12 , 80-233
Poland

Maciej Kahsin
e-mail: mkahsin@pg.edu.pl
Gdańsk University of Technology,
Gabriela Narutowicza Street 11/12 , 80-233
Poland